THE JOURNAL OF BIOLOGICAL CHEMISTRY
Vol. 277, No. 37, Issue of September 13, pp. 33913–33921, 2002

Printed in U.S.A.

The Consequence of Sequence Alteration of an Amphipathic α-Helical Antimicrobial Peptide and Its Diastereomers*

Received for publication, May 20, 2002, and in revised form, July 3, 2002
Published, JBC Papers in Press, July 10, 2002, DOI 10.1074/jbc.M204928200

Niv Papo‡, Ziv Oren‡, Ulrike Pag§, Hans-Georg Sahl§, and Yechiel Shai‡¶

From the ‡Department of Biological Chemistry, The Weizmann Institute of Science, Rehovot, 76100 Israel and the §Institute for Medical Microbiology and Immunology, University of Bonn, Sigmund-Freud-Strasse 25, D-53127 Bonn, Germany

The search for antibiotics with a new mode of action led to numerous studies on antibacterial peptides. Most of the studies were carried out with L-amino acid peptides possessing amphipathic α-helix or β-sheet structures, which are known to be important for biological activities. Here we compared the effect of significantly altering the sequence of an amphipathic α-helical peptide (15 amino acids long) and its diastereomer (composed of both L- and D-amino acids) regarding their structure, function, and interaction with model membranes and intact bacteria. Interestingly, the effect of sequence alteration on biological function was similar for the L-amino acid peptides and the diastereomers, despite some differences in their structure in the membrane as revealed by attenuated total reflectance Fourier-transform infrared spectroscopy. However, whereas the all L-amino acid peptides were highly hemolytic, had low solubility, lost their activity in serum, and were fully cleaved by trypsin and proteinase K, the diastereomers were nonhemolytic and maintained full activity in serum. Furthermore, sequence alteration allowed making the diastereomers either fully, partially, or totally protected from degradation by the enzymes. Transmembrane potential depolarization experiments in model membranes and intact bacteria indicate that although the killing mechanism of the diastereomers is via membrane perturbation, it is also dependent on their ability to diffuse into the inner bacterial membrane. These data demonstrate the advantage of the diastereomers over their all L-amino acid counterparts as candidates for developing a repertoire of new target antibiotics with a potential for systemic use.

The widespread use of antibiotics led to the development of numerous antibiotic-resistant strains, resulting in an urgent need for new antibiotics (1–4). The search for antibiotics with a new mode of action has increased the interest in antibacterial peptides as potential therapeutic agents. Isolation from biological sources (bacteria, insects, amphibians, mammals, etc.) has served as a common means for discovering novel antibacterial peptides such as gramicidins, magainins, defensins, cecropins, dermaseptins, and indolicidins (5–9). The amphipathic α-helix or β-sheet structures and a net positive charge are common characteristics found to be crucial for most native antibacterial peptides that act by perturbing the barrier function of membranes (3, 10–12). These features were used as building blocks to modify native sequences as well as to create many *de novo* designed antimicrobial peptides (13–20). Another important group of peptide antibiotics composed of both L- and D-amino acids includes gramicidins, actinomycins, bacitracin, lantibiotics, and bombinins H 3–5 (21–24). The coexistence of L- and D-amino acids causes the formation of unique structures and properties completely different from all L-amino acid peptides. Unfortunately, these peptide antibiotics are not cell-selective and are highly toxic to normal eukaryotic cells. Furthermore, their activity is significantly altered by the modification of sequences.

Previous studies revealed that the incorporation of D-amino acids into native and model non-cell-selective lytic peptides with either α-helix or β-sheet structures resulted in a loss of their cytotoxic effect on mammalian cells, but they retained their antibacterial properties (25, 26). All studies on their mode of action were carried out with diastereomers that possess an amphipathic structure, assuming that it plays an important role similar to what has been reported with native L-amino acid antimicrobial peptides (6–9). In this study we significantly altered the sequence of an α-helical lytic peptide (15 amino acids long) and its diastereomers. The peptides are composed of leucine and lysine, whereas one-third of the sequence of the diastereomers consists of D-amino acids. Peptide length and the position of D-amino acids were such that short consecutive stretches of 1–3 L-amino acids that cannot form an α-helical structure were constructed. Three peptides were designed to fold into an ideal amphipathic α-helix in their all L-amino acid form (*i.e.* the hydrophobic and hydrophilic amino acids are localized in opposite faces of the helix) but with a different distribution of the D-amino acids along the hydrophobic and hydrophilic faces; one had a scrambled sequence of hydrophobic and hydrophilic amino acids, and in two peptides we grouped the hydrophobic and hydrophilic amino acids (termed segregated peptides). The diastereomers and their representative all L-amino acid parental peptides were evaluated with regard to their cytotoxicity against bacteria and human erythrocytes, their structure in phospholipid membranes, their ability to depolarize the transmembrane potential of bacteria and model phospholipid vesicles, their ability to oligomerize in solution and in membranes, and their stability regarding enzymatic degradation. We discuss the results with respect to the mode of action of diastereomeric peptides and their advantage over their all L-amino acid counterparts for future therapeutic use.

EXPERIMENTAL PROCEDURES

Materials

4-Methyl benzhydrylamine resin and butyloxycarbonyl amino acids were purchased from Calibochem-Novabiochem (La Jolla, CA). Other reagents used for peptide synthesis included trifluoroacetic acid (Sigma), *N*,*N*-diisopropylethylamine (Aldrich), methylene chloride (peptide

* This work was supported by the European Community Project Number QLK2-2000-00411. The costs of publication of this article were defrayed in part by the payment of page charges. This article must therefore be hereby marked "*advertisement*" in accordance with 18 U.S.C. Section 1734 solely to indicate this fact.

¶ The Harold S. and Harriet B. Brady Professorial Chair in Cancer Research. To whom correspondence should be addressed. Tel.: 972-8-9342711; Fax: 972-8-9344112; E-mail: Yechiel.Shai@weizmann.ac.il.

synthesis grade, Biolab, IL), dimethylformamide (peptide synthesis grade, Biolab, IL), piperidine (Merck), and benzotriazolyl-*n*-oxy-tris-(dimethylamino)phosphonium-hexafluorophosphate (Sigma). Trypsin, proteinase K, egg phosphatidylcholine (PC),[1] egg phosphatidylglycerol (PG), phosphatidylethanolamine (PE) (Type V, from *E. coli*), sphingomyelin (SM), and cholesterol were purchased from Sigma. 3,3′-Diethylthio-dicarbocyanine iodide (diS-C_3-5) was obtained from Molecular Probes (Eugene, OR). All of the other reagents were of analytical grade. The buffers were prepared in double glass-distilled water.

Peptide Synthesis and Purification

The peptides were synthesized by a solid phase method on 4-methyl benzhydrylamine resin (0.05 meq) (27). Labeling of the N terminus of the peptides with rhodamine was done on the resin-bound peptide as described previously (18). The resin-bound peptides were cleaved from the resins by hydrogen fluoride and, after hydrogen fluoride evaporation and washing with dry ether, extracted with 50% acetonitrile/water. Hydrogen fluoride cleavage of the peptides bound to 4-methyl benzhydrylamine resin resulted in C-terminally amidated peptides. Each crude peptide contained one major peak, as revealed by RP-HPLC that was 50–70% pure by weight. The peptides were further purified by RP-HPLC on a C_{18} reverse phase Bio-Rad semi-preparative column (250 × 10 mm, 300-Å pore size, 5-μm particle size). The column was eluted in 40 min using a linear gradient of 10–60% acetonitrile in water, both containing 0.05% trifluoroacetic acid (v/v), at a flow rate of 1.8 ml/min. The purified peptides were shown to be homogeneous (>98%) by analytical HPLC. The peptides were further subjected to amino acid analysis and electrospray mass spectroscopy to confirm their composition and molecular weight.

Preparation of Small (SUV) and Large (LUV) Unilamellar Vesicles

SUVs were prepared by sonication of PC/SM/cholesterol (5:5:1 w/w) or PE/PG (7:3 w/w) dispersions as described previously (17). LUVs were prepared by extrusion from the same lipids as described in detail previously (28). The vesicles were visualized using a JEOL JEM 100B electron microscope (Japan Electron Optics Laboratory Co., Tokyo, Japan) as follows. A drop of the vesicles was deposited on a carbon-coated grid and negatively stained with uranyl acetate. Examination of the grids showed that the vesicles were unilamellar with an average diameter of 20–50 nm with SUV and 100 nm with LUV.

Antibacterial Activity of the Peptides

The antibacterial activity of the peptides was examined in sterile 96-well plates (Nunc F96 microtiter plates) in a final volume of 100 μl as follows. Aliquots (50 μl) of a suspension containing bacteria (mid-log phase) at a concentration of 10^6 colony-forming units/ml in culture medium (LB medium) were added to 50 μl of water containing the peptide in serial 2-fold dilutions in water. Inhibition of growth was determined by measuring the absorbance at 600 nm with a Microplate autoreader El309 (Bio-tek Instruments) after an incubation of 18–20 h at 37 °C. The antibacterial activities were expressed as the minimal inhibitory concentration (MIC), the concentration at which 100% inhibition of growth was observed after 18–20 h of incubation. The bacteria used were *Escherichia coli* D21, *E. coli* ATCC 25922, *Acinetobacter baumannii* ATCC 19606, *Pseudomonas aeruginosa* ATCC 27853, *Micrococcus luteus*, *Staphylococcus aureus* ATCC 5185, as well as two clinical isolates, *Staphylococcus simulans* 22 and methicillin-resistant *Staphylococcus epidermidis* LT1324.

Hemolysis of Human Red Blood Cells (hRBCs)

Fresh hRBCs were rinsed three times with PBS (35 mM phosphate buffer, 0.15 M NaCl, pH 7.3) by centrifugation for 10 min at 800 × *g* and resuspended in PBS. The peptides dissolved in PBS were then added to 50 μl of the stock hRBC solution in PBS to make a final volume of 100 μl (final erythrocyte concentration, 4% v/v). The resulting suspension was incubated with agitation for 60 min at 37 °C. The samples were then centrifuged at 800 × *g* for 10 min. By measuring the absorbance of the supernatant at 540 nm, we monitored the release of hemoglobin. Controls for zero hemolysis (blank) and 100% hemolysis consisted of hRBCs suspended in PBS and 1% Triton X-100, respectively.

Increase in Membrane Permeability Induced by the Peptides

Membrane destabilization, which results in the collapse of the diffusion potential, was detected fluorimetrically as described previously (29–31). Briefly, a LUV suspension prepared in K^+ buffer (50 mM K_2SO_4, 25 mM HEPES-sulfate, pH 6.8) was added to an isotonic K^+-free buffer (50 mM Na_2SO_4, 25 mM of HEPES-sulfate, pH 6.8), and the dye diS-C_3-5 was then added. The subsequent addition of valinomycin created a negative diffusion potential inside the vesicles by the selective efflux of K^+ ions, which resulted in quenching of the dye fluorescence ($\Delta\Psi = -142$ mV). Peptide-induced membrane permeation for all of the ions in the solution caused a dissipation of the diffusion potential, manifested by an increase in fluorescence. The fluorescence was monitored using excitation and emission wavelengths at 620 and 670 nm, respectively. The percentage of fluorescence recovery (F_t) was defined by the following equation,

$$F_t = [(I_t - I_o)/(I_f - I_o)]100\% \quad \text{(Eq. 1)}$$

where I_t is the fluorescence observed after the addition of a peptide at time t, I_o is the fluorescence after the addition of valinomycin, and I_f is the total fluorescence before adding valinomycin.

Transmembrane Potential Depolarization Assay with Bacteria

The assay was done with Gram-negative bacterial spheroplasts and Gram-positive bacteria, using the experimental conditions described previously (32).

Gram-positive Bacteria—S. aureus was grown at 37 °C with agitation to mid-log phase (OD_{600} = 0.4). The cells were centrifuged and washed once with buffer (20 mM glucose, 5 mM HEPES, pH 7.3) and resuspended to a OD_{600} of 0.05 in a similar buffer containing 0.1 M KCl. The cells (the same concentration as in the biological activity assay) were incubated with 1 μM diS-C_3-5 until a stable reduction of fluorescence was achieved (around 60 min), indicating the incorporation of the dye into the bacterial membrane. The peptides were then added from the stock solution (1 mg/ml) and dissolved in the KCl buffer to achieve the desired concentration (0.1–10-fold the MIC concentration). Membrane depolarization was monitored by observing the change in the intensity of fluorescence emission of the membrane potential-sensitive dye diS-C_3-5 (excitation wavelength λ_{ex} = 622 nm, emission wavelength λ_{em} = 670 nm) after the addition of different concentrations of peptides.

Gram-negative Bacteria—Spheroplasts of *E. coli* (D21 and ATCC 25922 strains) (lipopolysaccharide and peptidoglycane free bacteria (33)) were prepared by osmotic shock procedure as follows. First, the cells from cultures grown to OD_{600} = 0.8 were harvested by centrifugation and washed twice with 10 mM Tris/H_2SO_4, 25% sucrose, pH 7.5. Next, the cells were resuspended in the washing buffer containing 1 mM EDTA. After a 10-min incubation at 20 °C with rotary mixing, the cells were collected by centrifugation and resuspended immediately in freezing (0 °C) water. After a 10-min incubation at 4 °C with rotary mixing, the spheroplasts were collected by centrifugation. The spheroplasts were then resuspended to OD_{600} of 0.05 in a buffer containing 20 mM glucose, 5 mM HEPES, 1 M KCl, pH 7.3. Further treatment was done exactly as described for *S. aureus*.

ATR-FTIR Measurements

The spectra were obtained with a Bruker equinox 55 FTIR spectrometer equipped with a deuterated triglyceride sulfate detector and coupled to an ATR device as described previously (34). Briefly, a mixture of PE/PG (0.5 mg) alone or with peptide (~20 μg) was deposited on a ZnSe horizontal ATR prism (80 × 7 mm). The aperture angle of 45° yielded 25 internal reflections. Prior to sample preparations, the trifluoroacetate (CF_3COO^-) counterions, which strongly associate with the peptides, were replaced with chloride ions through several lyophilizations of the peptides in 0.1 M HCl to eliminate an absorption band near 1673 cm^{-1} (35). Lipid-peptide mixtures were prepared by dissolving them together in a 1:2 MeOH/CH_2Cl_2 mixture and drying under a stream of dry nitrogen while moving a Teflon bar back and forth along the ZnSe prism. The spectra were recorded, and the respective pure phospholipid spectra were subtracted to yield the difference spectra. The background for each spectrum was a clean ZnSe prism. Hydration of the sample was achieved by introducing excess deuterium oxide (^2H_2O) into a chamber placed on top of the ZnSe prism in the ATR casting and incubating for 2 h before acquisition of the spectra. The H/D (proton to deuterium)

[1] The abbreviations used are: PC, egg phosphatidylcholine; ATR, attenuated total reflectance; FTIR, Fourier transform infrared; diS-C_3-5, 3,3′-diethylthiodicarbocyanine iodode; hRBC, human red blood cells; LUV, large unilamellar vesicle; SUV, small unilamellar vesicle; MIC, minimal inhibitory concentration; PBS, phosphate buffered saline; PE, *E. coli* phosphatidylethanolamine; PG, egg phosphatidylglycerol; SM, sphingomyelin; RP-HPLC, reverse phase high performance liquid chromatography.

TABLE I
Designations, sequences, retention times, and percentages of enzymatic degradation of the peptides investigated

Peptide designation	Sequence[a]	RP-HPLC retention time	Enzymatic degradation[b]
		min	*%*
L-Amino acid peptides			
Amphipathic-1L	LKLLKKLLKKLLKLL-NH_2	24.23	100
Scrambled-4L	KLKLLKLLKLLKLLK-NH_2	24.41	100
Segregated-5L	KKKLLLLLLLLLKKK-NH_2	23.30	100
Diastereomers			
Amphipathic-1D	LK**L**LK**K**L**L****K**KLL**K**LL-NH_2	22.95	58
Amphipathic-2D	LL**K**KL**L**K**L****L**LKL**L**KK-NH_2	23.12	100
Amphipathic-3D	LL**K**LL**K**K**L****L**KKL**L**KL-NH_2	21.31	100
Scrambled-4D	KL**K**LL**K**L**L****K**LLK**L**LK-NH_2	23.02	26
Segregated-5D	KK**K**LL**L**L**L****L**LLL**K**KK-NH_2	25.05	0
Segregated-6D	LL**L**LL**K**K**K****K**KKL**L**LL-NH_2	26.98	100

[a] Underlined and bold amino acids are D-enantiomers. All of the peptides are amidated in their C terminus.
[b] The peptides were treated for 2 h with trypsin or proteinase K.

exchange was considered complete after total shift of the amide II band. Any contribution of ^2H_2O vapor to the absorbance spectra near the amide I peak region was eliminated by subtracting the spectra of pure lipids equilibrated with ^2H_2O under the same conditions.

ATR-FTIR Data Analysis

Prior to curve fitting, a straight base line passing through the ordinates at 1700 and 1600 cm^{-1} was subtracted. To resolve overlapping bands, the spectra were processed using PEAKFIT™ (Jandel Scientific, San Rafael, CA) software. Second-derivative spectra accompanied by 13-data point Savitsky-Golay smoothing were calculated to identify the positions of the component bands in the spectra. These wave numbers were used as initial parameters for curve fitting with Gaussian component peaks. Position, bandwidths, and amplitudes of the peaks were varied until (i) the resulting bands shifted by no more than 2 cm^{-1} from the initial parameters, (ii) all of the peaks had reasonable half-widths ($< 20–25$ cm^{-1}), and (iii) good agreement between the calculated sum of all of the components and the experimental spectra was achieved ($r^2 > 0.99$). The relative contents of different secondary structure elements were estimated by dividing the areas of individual peaks assigned to a specific secondary structure by the whole area of the resulting amide I band. The results of four independent experiments were averaged.

CD Spectroscopy

The CD spectra of the peptides were measured with a Jasco J-500A spectropolarimeter after calibrating the instrument with (+)-10-camphorsulfonic acid. The spectra were scanned at 25 °C in a capped, quartz optical cell with a 0.5 mm path length. The spectra were obtained at wavelengths of 250–190 nm. Eight scans were taken for each peptide at a scan rate of 20 nm/min. The peptides were scanned at 50 μM in the presence of 1% SDS. Fractional helicities (36, 37) were calculated as follows,

$$\frac{[\theta]_{222} - [\theta]^0_{222}}{[\theta]^{100}_{222} - [\theta]^0_{222}} \qquad \text{(Eq. 2)}$$

where $[\theta]_{222}$ is the experimentally observed mean residue ellipticity at 222 nm, and the values for $[\theta]^0_{222}$ and $[\theta]^{100}_{222}$, which correspond to 0 and 100% helix content at 222 nm, are estimated to be 2000 and 32000 deg·cm^2/dmol, respectively (37).

Enzymatic Degradation

Trypsin or proteinase K (10 μg/ml in PBS) was added to a solution of the peptides in PBS (1 μM), and the reaction was monitored by using RP-HPLC and electrospray mass spectroscopy. We used RP-HPLC with a C_{18} reverse phase Bio-Rad analytical column (250 × 4 mm, 300-Å pore size, 7-μm particle size). The column was eluted in 40 min, using a linear gradient of 10–60% acetonitrile in water both containing 0.05% trifluoroacetic acid (v/v) at a flow rate of 0.6 ml/min. The electrospray mass spectroscopy was performed to confirm the composition and molecular weight of the product.

Oligomerization of the Peptides in Solution and in the Phospholipid Membrane as Determined by Rhodamine Fluorescence Dequenching Measurements

Rhodamine-labeled peptide (final concentration, 2 μM) was added to 100 μl of PBS, PC/SM/cholesterol (5:5:1 w/w), and PE/PG (7:3 w/w) SUVs, and rhodamine fluorescence emission was tracked. Lipid concentration was kept high (100 μM) such that most of the peptide was bound to the vesicles. Trypsin or proteinase K (10 μg/ml in PBS) was then added, and the resulting fluorescence was monitored. An increase in fluorescence indicates that the peptide exists as an oligomer. Excitation was set at 530 nm (8-nm slit) and emission was set at 582 nm (4-nm slit). All of the fluorescence measurements were performed at room temperature on an SLM-Aminco Series 2 Spectrofluorimeter.

Examination of Bacterial Membrane Damage by Electron Microscopy

The samples containing *E. coli* D21 and *P. aeruginosa* ATCC 27853 (1×10^6 colony-forming units/ml) in LB medium were incubated with the peptides at their MIC and 60% of the MIC for 1 h and then centrifuged for 10 min at 300 × *g*. The pellets were resuspended, and a drop containing the bacteria was deposited onto a carbon-coated grid and negatively stained with 2% phosphotungstic acid, pH 6.8. The grids were examined using a JEOL JEM 100B electron microscope (Japan Electron Optics Laboratory Co., Tokyo, Japan).

RESULTS

The data presented in the following sections revealed that the all L-amino acid parental peptides are highly hemolytic, are fully cleaved by enzymes, and lose their activity in serum and that some have low solubility in water. In contrast, all of the diastereomers are nonhemolytic, their sensitivity to enzymatic degradation can be controlled, they are highly soluble in water, and they maintain full activity in serum. Therefore, beside determination of structure, which was done for both the all L-amino acid peptides and the diastereomers, all of the other biophysical studies were carried out only with the diastereomers.

Peptide Design—The six diastereomers of a lytic peptide and three representatives of the all L-amino acid counterparts were composed of lysine and leucine. All of the peptides were amidated at their C termini and had a net +7 charge. The amino acid sequences of the peptides, as well as their designations and retention times are shown in Table I. Fig. 1 shows a Schiffer-Edmundson (38) wheel structure of the amphipathic all L-amino acid peptide, Amphipathic-1L (Fig. 1*A*), as well as those of the corresponding amphipathic diastereomers to visualize the distribution of the D-amino acids (Fig. 1, *B–D*). The amphipathic diastereomers also have a markedly α-helical/distorted helical structure (to be discussed later). D-Amino acids were located in all of the peptides at positions 3, 6, 8, 9, and 13, which are likely to disrupt the formation of a helical structure. Among the diastereomers, the distribution of the D-amino acids along the hydrophobic and hydrophilic faces is different (Fig. 1, *B–D*). Other peptides include a scrambled all L-amino acid peptide and its diastereomer, as well as one all L-amino acid peptide and its two diastereomers, in which the hydrophobic and hydrophilic amino acids were grouped (segregated peptides).

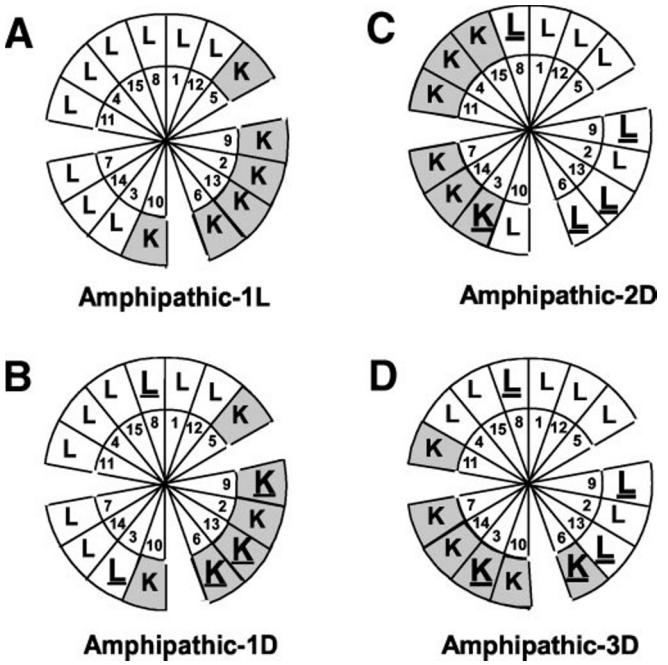

FIG. 1. **Schiffer-Edmundson wheel projection (38) of the peptides.** The *gray shading* indicates hydrophilic amino acids (Lys). *No shading* indicates hydrophobic amino acid (Leu), and the *underlined letters* indicate hydrophobic and hydrophilic D-amino acids.

Antimicrobial Activities of the Peptides in Buffer and Serum and Their Hemolytic Activity—Antibacterial activity was assayed against a representative set of test bacteria including both Gram-negative and Gram-positive species. Table II summarizes the results. Interestingly, the trend in antimicrobial activity was similar for the all L-amino acid peptides and their corresponding diastereomers. In addition, the amphipathic diastereomers, 1D, 2D, and 3D, had a similar high antimicrobial activity against all bacteria tested, despite a different distribution of the D-amino acids along the amphipathic face (Fig. 1, *B–D*). Furthermore, even scrambling the sequence did not significantly change the activity of the resulting analogs. In addition, segregating the hydrophilic and hydrophobic amino acids also preserved activity but only toward selected bacteria (Table II).

Antimicrobial activity was also measured in the presence of 30% human serum. The data revealed that the diastereomers had MIC values similar to those determined in buffer and therefore are not shown. In contrast, all of the L-amino acid peptides lost their activity. None of them was active at a concentration of up to 100 μM, the maximum concentration tested. Furthermore, some of the all L-amino acid peptides became highly aggregated in PBS (visualized as a cloudy solution), and therefore their stock solution had to be prepared by dissolving them in Me_2SO.

The peptides were also tested for their hemolytic activity against the highly sensitive human erythrocytes. Table II shows that the all L-amino acid peptides are highly hemolytic, whereas the diastereomers are devoid of hemolytic activity up to 100 μM, the maximum concentration tested.

Increase in Membrane Permeability Induced by the Diastereomeric Peptides—Dissipation of diffusion potential experiments were used to test whether the alteration of the sequence of the diastereomer reduced the ability of the analogs to increase the permeability of LUVs composed of phospholipids that mimic the composition of *E. coli* (PE/PG, 7:3 w/w) and erythrocyte membranes (PC/SM/cholesterol, 5:5:1 w/w/w) (39). The diastereomers were mixed at various concentrations with vesicles and pretreated with the fluorescent dye diS-C_3-5 and valinomycin. Fluorescence recovery over time was used to measure the kinetics of dissipation of the diffusion potential induced by the peptides. We also determined the maximum recovery level reached as a function of the lipid-to-peptide molar ratio. Unexpectedly, the data revealed that all of the diastereomers have similar activity in increasing the permeability of PE/PG membranes (Fig. 2*A*), despite major differences in the distribution of amino acids along the peptide chain. However, these results are not fully correlated with the antibacterial activity of the peptides, which sometimes show large differences between the peptides. Furthermore, besides Segregated-6D, the activities of the peptides toward zwitterionic membranes (PC/SM/cholesterol; Fig. 2*B*) were only slightly lower than their activities toward the negatively charged PE/PG membranes. Despite this, all of the peptides were not hemolytic, indicating that factors other than pure peptide-lipid interactions are involved in the biological activity of this group of diastereomeric peptides (discussed in the next section).

Depolarization of the Membrane Potential of Bacteria—To test whether factors other than the ability to interact with the bacterial membrane are important for antimicrobial activity, we performed transmembrane potential depolarizing experiments with Gram-negative bacteria spheroplasts. We used a sensitive strain (*E. coli* D21) and a less sensitive strain (ATCC 25922). In addition we used intact Gram-positive bacteria (*S. aureus*). The conditions were similar to what was reported previously using a mutant of *E. coli* DC2 with increased membrane permeability (32). The cell concentrations in the diffusion potential assay were similar to the ones used in the antimicrobial assay. Fig. 3 shows the dose-dependent dissipation of the transmembrane potential of *S. aureus*, and Fig. 4 shows that of *E. coli* D21 and ATCC 25922 spheroplasts, respectively. The data reveal a direct correlation between the MIC values for *S. aureus* and the dose-dependent dissipation of transmembrane bacterial potential, suggesting that a major target of these peptides is the bacterial plasma membrane. However, despite differences in the MIC values for the D21 and ATCC 25922 strains of *E. coli*, all of the diastereomeric peptides possess similar activities in the dissipation of the transmembrane potential of these two bacterial strains. These data correlate with similar activities of the peptides in the dissipation of the diffusion potential of PE/PG membranes. It is therefore reasonable to deduce that the major target of the peptides is the inner membrane of the bacteria and that the differences in their MIC values may result from differences in their ability to penetrate through the bacterial cell wall into the inner cytoplasm membrane. The alteration in the distribution of the amino acids affected the structure of the peptides and therefore also their ability to diffuse into the inner membrane via a process described as self-promoted uptake (40). Note, however, that the depolarization assay is done in PBS, whereas the antimicrobial assay is done in LB medium. Furthermore, whereas the antimicrobial assay proceeds for 18–20 h at 37 °C, the dissipation of the bacterial membrane potential is performed up to 60 min at 25 °C.

Stability of the Peptides to Enzymatic Degradation—The peptides were treated for 2 h with trypsin or proteinase K, and the solution was analyzed using RP-HPLC and mass spectroscopy as described under "Experimental Procedures." The data reveal that the diastereomeric Amphipathic-2D, Amphipathic-3D, and Segregated-6D were fully degraded (Table I). In contrast, no degradation was observed with Segregated-5D. Furthermore, Amphipathic-1D and Scrambled-4D were only partially degraded (58 and 26%, respectively). Similar results were found with both enzymes. In contrast, the all L-amino acid peptides were degraded completely by the enzymes. These data

TABLE II
Minimal inhibitory concentrations of the peptides and their hemolytic activity

Peptide designation	*E. coli* ATCC 25922	*E. coli* D21	MRSE LT1324[a]	*P. aeruginosa* ATCC 27853	*A. baumannii* ATCC 19606	M. luteus	S. simulans	*S. aureus* II ATCC 6538P	Hemolysis at 100 μM
	μM	μM	μM	μM	μM	μM	μM	μM	%
L-Amino acid peptides									
Amphipathic-1L	13	13	4	25	1	2	2	3	100
Scrambled-4L	3	3	1.5	6	2	2	1.5	6	82
Segregated-5L	50	50	32	>50	50	16	32	50	66
Diastereomers									
Amphipathic-1D	7	4	1	3	13	0.5	1	13	0
Amphipathic-2D	22	6	0.5	6	11	0.5	1	25	0
Amphipathic-3D	11	5	1	3	10	0.5	1	45	0
Scrambled-4D	6	3	1	6	15	0.4	1	25	0
Segregated-5D	44	14	1	50	50	0.3	1	>50	3
Segregated-6D	>56	7	1	8	50	0.5	1	>50	0

[a] MRSE, methicillin-resistant *S. epidermidis*.

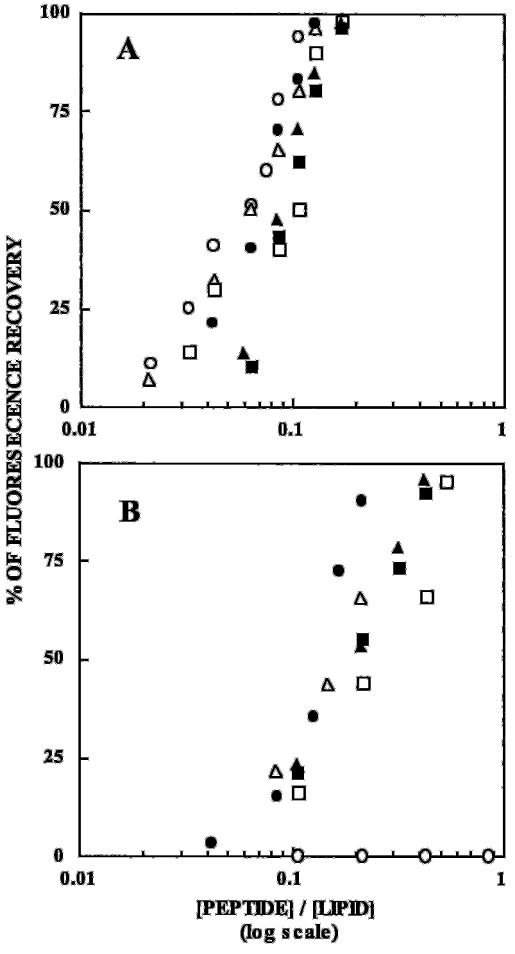

FIG. 2. **Maximal dissipation of the diffusion potential in vesicles, induced by the diastereomeric peptides.** The diastereomers were added to isotonic K^+-free buffer containing LUVs composed of PE/PG (*A*) or PC/SM/cholesterol (*B*), pre-equilibrated with the fluorescent dye diS-C_2-5 and valinomycin. Fluorescence recovery was measured 3–10 min after the peptides were mixed with the vesicles. ▲, Amphipathic-1D; ■, Amphipathic-2D; ●, Amphipathic-3D; □, Scrambled-4D; △, Segregated-5D; ○, Segregated-6D.

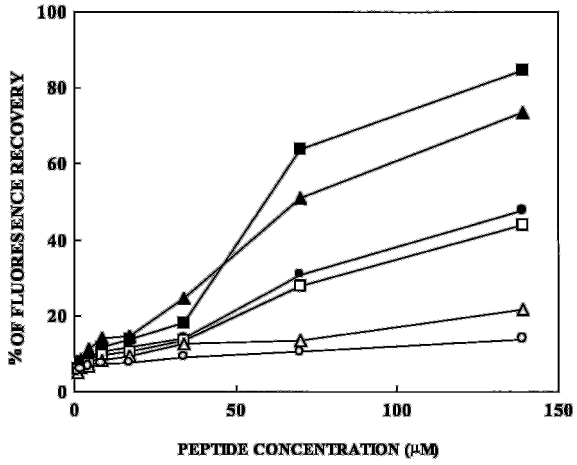

FIG. 3. **Maximal dissipation of the diffusion potential in bacterial membrane, induced by the diastereomeric peptides.** The diastereomers were added to *S. aureus* bacteria that were pre-equilibrated with the fluorescent dye diS-C_2-5 for 60 min. Fluorescence recovery was measured 1–120 min (at 5-min intervals) after the peptides were mixed with the bacteria, and its maxima was reported. ▲, Amphipathic-1D; ■, Amphipathic-2D; ●, Amphipathic-3D; □, Scrambled-4D; △, Segregated-5D; ○, Segregated-6D.

reveal an important advantage of the diastereomers, in which sensitivity to enzymatic degradation can be controlled.

Oligomerization of the Peptides in Aqueous Solution and Phospholipid Membranes as Determined by Rhodamine Dequenching Experiments—The fluorescence of rhodamine is only slightly sensitive to the polarity of its environment and therefore can be studied in aqueous solution and membranes. The attachment of rhodamine to the N terminus of the peptides did not affect their antimicrobial activity (data not shown). When rhodamine-labeled monomers are self-associated and the rhodamine probes are in close proximity, the result is self-quenching of the emission fluorescence. A 5–10-fold difference in the fluorescence intensity of a peptide treated with a proteolytic enzyme and that of an untreated peptide determines whether the peptide is self-associated or not (41). Some of the peptides were fully cleaved by the enzymes and others were not (Table I). The following results suggest that all of the diastereomers are not oligomerized in solution or in the membrane: (i) the finding that the fluorescence of a rhodamine-labeled diastereomer (which is sensitive to degradation) dissolved at 2 μM in PBS reached similar levels before or after its enzymatic degradation or when bound to the membrane is similar (~0.1–0.3-fold difference) (data not shown); (ii) the finding of a similar final level of fluorescence for all of the diastereomers, whether they are cleaved or not cleaved by the enzymes; and (iii) the fact that all of the diastereomers were used at the same 2 μM concentration. These data reveal that differences in antimicrobial activity between the diastereomers are not the result of differences in their oligomeric state. The oligomeric state in membrane and solution have been previously shown to affect antimicrobial activity (19, 26, 41, 42).

Secondary Structure of the Peptides in PE/PG Phospholipid Membrane as Determined by FTIR Spectroscopy—FTIR spectroscopy was used to determine the secondary structure of the peptides (all L-amino acid and diastereomeric peptides) within

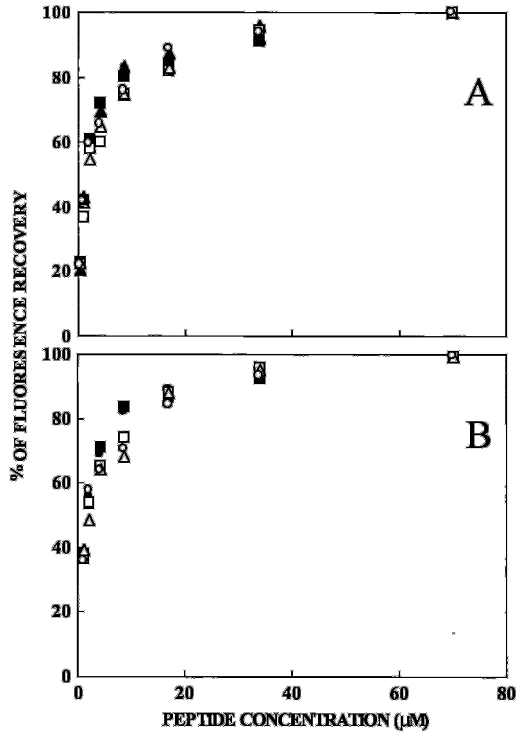

FIG. 4. **Maximal dissipation of the diffusion potential in bacterial membrane, induced by the diastereomeric peptides.** The diastereomers were added to spheroplasts of sensitive *E. coli* D21 (*A*) or spheroplasts of less sensitive *E. coli* ATCC 25922 (*B*) that were pre-equilibrated with the fluorescent dye diS-C_2-5 for 60 min. Fluorescence recovery was measured 1–120 min (at 5-min intervals) after the peptides were mixed with the bacteria, and its maxima was reported. ▲, Amphipathic-1D; ■, Amphipathic-2D; ●, Amphipathic-3D; □, Scrambled-4D; △, Segregated-5D; ○, Segregated-6D.

the phospholipid membrane. Helical and unordered structures can contribute to the amide I vibration at almost identical wave numbers, and it is difficult to determine the precise proportion of helix and random coil from the IR spectra. However, the exchange of hydrogen with deuterium makes it sometimes possible to differentiate α-helical components from random structure, because the absorption of the random structure shifts to a higher extent than the α-helical component after deuteration. Therefore, we examined the IR spectra of the peptides after complete deuteration. The amide I region spectra of the diastereomeric peptides Amphipathic-2D and Segregated-5D bound to PE/PG (7:3 w/w) multibilayers are shown in Fig. 5 (*A* and *C*, respectively). Second derivatives, accompanied by 13-data point Savitsky-Golay smoothing, were calculated to identify the positions of the component bands in the spectra and are given in Fig. 5 (*B* and *D*). These wave numbers were used as initial parameters for curve fitting with gaussian component peaks. Assignment of the different secondary structures to the various amide I regions was calculated according to the values taken from Refs. 43 and 44 and our previous results (45–47). The assignments, wave numbers (υ), and relative areas of the component peaks are summarized in Table III for PE/PG (7:3 w/w). The amide I region from 1656 to 1670 cm^{-1} is characteristic of 3_{10}-helix or dynamic/distorted α-helix, as was previously suggested in a study that examined structural changes in phospholipase A_2 (48). The assignment of the amide I region from 1656 to 1670 cm^{-1} to dynamic helix is further supported by studies that examined distorted α-helical structures (α_{II}-helices) in bacteriorhodopsin and other proteins (49, 50). These studies demonstrated that distorted α-helical structures are characterized by increased amide I frequencies. The assignment of the amide I region between 1670 and 1680 cm^{-1} remains uncertain. Previous studies have correlated this region with β-turns (51), possibly sterically constrained non-hydrogen-bonded amide C=O groups within turns (52), or the high frequency β-sheet component (53), which arises as a consequence of a transition dipole coupling (54).

Interestingly, the data reveal some similarities between the structures of the all L-amino acid Amphipathic-1L and Scrambled-4L and their corresponding diastereomers when bound to PE/PG membrane. This might explain in part their similar antimicrobial activity.

Note that compared with the diastereomeric Amphipathic-2D and Amphipathic-3D, Amphipathic-1D does not have two consecutive hydrophobic D-amino acids, and therefore, most of the hydrophobic face contains L-amino acids (Table I and Fig. 1). Because hydrophobic interactions are responsible for the secondary structure in the membrane, they possibly stabilize the formation of a higher value of α-helix in Amphipathic-1D compared with the more distorted helix in the other two. Despite a differences in the distribution of Lys and Leu in the diastereomeric Segregated-5D and 6D, both have similar structures in PE/PG, which is about 30–40% α-helix and 30–45% aggregated β-sheet. The aggregated β-sheet band could result from peptide aggregation caused by intermolecular hydrophobic interactions between stretches of adjacent leucines that do not exist in the other peptides. Similar results were obtained when 1:60 and 1:120 peptide to lipid molar ratios were used.

Secondary Structure and Aggregation of the Peptides in SDS Solution as Examined by Circular Dichroism Spectroscopy—The secondary structure of the all L-amino acid peptides (50 μM) was determined in 1% SDS solution, a solution that mimics the membrane environment. We found that despite a major alteration of their sequences, the nonamphipathic peptides preserved a high level of α-helical content (Fig. 6). The values obtained are ~90%, 50%, and 47% α-helix for the all L-amino acid peptides Amphipathic-1L, Scrambled-4L, and Segregated-5L, respectively.

Electron Microscopy Visualization of Bacterial Lysis—The effect of the diastereomeric Amphipathic-1D on *E. coli* and *P. aeruginosa* was visualized using transmission electron microscopy. At concentrations corresponding to 60% of the MIC values, significant differences in the morphology of the treated bacteria were noted. More specifically, Amphipathic-1D caused initial damage to the cell wall and membrane of both *E. coli* (Fig. 7*B*) and *P. aeruginosa* (Fig. 7*E*). Furthermore, at the MIC, the diastereomer caused serious damage to both the *E. coli* and *P. aeruginosa* cell membranes (Fig. 7, *C* and *F*, respectively), however, with different morphologies. Segregated-5 was used as a control, and at the MIC of Amphipathic-1, no change in the morphology of *P. aeruginosa* was observed (Fig. 7*G*).

DISCUSSION

Linear antimicrobial peptides that form an amphipathic α-helical structure upon their binding to the bacterial membrane are among the most abundant and widespread in nature. Many studies have demonstrated that alteration of amphipathicity significantly reduces their potent, broad spectrum antimicrobial activity (3, 4, 9). Our results are discussed with respect to three interesting findings: (i) The antimicrobial activity of the all L-amino acid peptides, irrespective of sequence alteration, is similar to that of their corresponding diastereomers, and in both cases sequence alteration preserves full or partial antimicrobial activity. This can be partly explained by the similar structure in the membrane of the L-amino acid peptides and their counterpart diastereomers. (ii) The all L-amino acid peptides are highly hemolytic, fully degraded by trypsin and

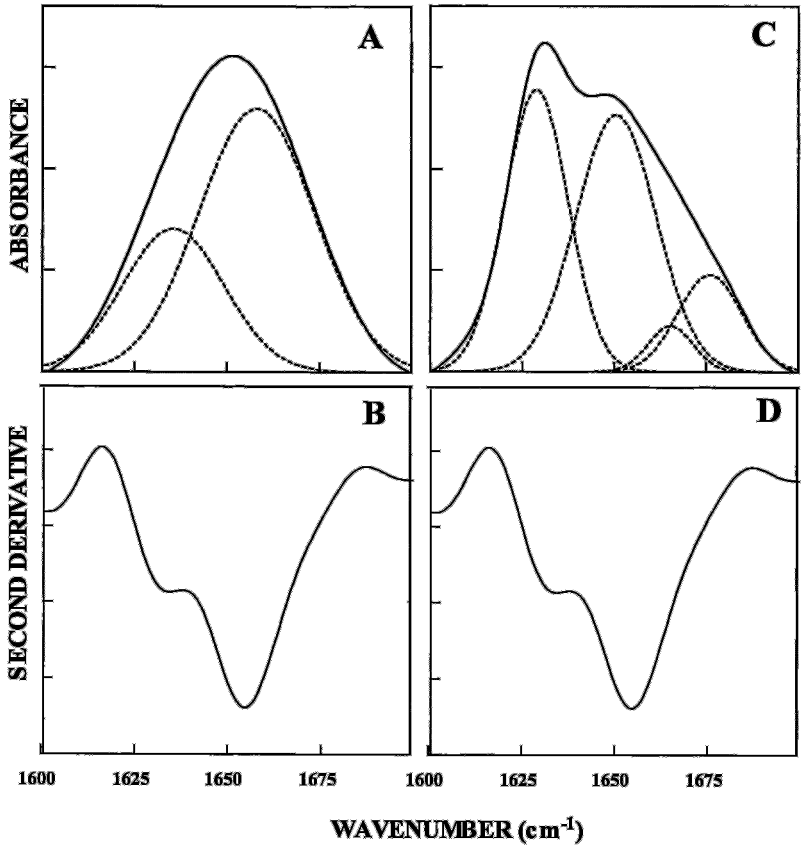

FIG. 5. **FTIR spectra deconvolution of the fully deuterated amide I band (1600–1700 cm^{-1}) of Amphopathic-2D (*A*) and segregated-5D (*C*) diastereomers in PE:PG (7:3 w/w) multibilayers.** Second derivatives (*lower panels*) were calculated to identify the positions of the component bands in the spectra. The component peaks are the result of curve fitting using a Gaussian line shape. The sums of the fitted components superimpose on the experimental amide I region spectra. The *solid lines* represent the experimental FTIR spectra after Savitzky-Golay smoothing; the *dashed lines* represent the fitted components. A 120:1 lipid/diastereomer molar ratio was used.

TABLE III
Peptide structure as determined by ATR-FTIR spectroscopy from the deconvolution of the Amide I bands of the all L and the diastereomeric peptides incorporated into PE:PG multibilayers

A 120:1 lipid:peptide molar ratio was used. The results are the averages of four independent experiments.

Peptide designation	β-Sheet + aggregated strands	Random coil/α-helix	Distorted/ 3_{10}-helix
	%	%	%
L-Amino acid peptides			
Amphipathic-1L		79 ± 2	21 ± 2
Scrambled-4L	71 ± 1	29 ± 3	
Segregated-5L	70 ± 2	30 ± 2	
Diastereomers			
Amphipathic-1D	17 ± 3	43 ± 2	40 ± 3
Amphipathic-2D	33 ± 4		67 ± 4
Amphipathic-3D	32 ± 3		68 ± 3
Scrambled-4D	38 ± 5		62 ± 2
Segregated-5D	57 ± 3	36 ± 6	7 ± 1
Segregated-6D	39 ± 7	30 ± 5	31 ± 5

proteinase K, and inactivated in serum; some have low solubility in water. In contrast, all of the diastereomers are nonhemolytic, their sensitivity to enzymatic degradation can be controlled, they are highly soluble in water, and they maintain full activity in serum. (iii) Despite major sequence alteration, all of the diastereomeric peptides have similar potency in permeating phospholipid membranes, as well as the inner bacterial membrane. This may indicate that the differences in their antimicrobial activities are the result of a different ability to diffuse through the outer layer into the inner phospholipid membrane (elaborated in the next paragraphs).

Sequence alteration was achieved by three types of modifications: (i) The positions of the D-amino acids were changed without alteration of the amphipathic organization (*i.e.* Amphipathic-1D, -2D, and -3D). Interestingly, these modifications did not significantly alter the potency and the spectrum of activity of the resulting analogs, which suggests that once a potent peptide is designed, the position of the D-amino acids can be changed to produce a repertoire of new active compounds that differ from each other by their structure (and hence should have different antigenicities) and by their susceptibility to enzymatic degradation. For example, Amphipathic-1D has a slightly different structure than Amphipathic-2D and -3D and becomes more resistant to proteolytic degradation by trypsin and proteinase K. Note that lytic peptides that are fully degraded or fully protected from enzymatic degradation are not suitable for systemic use in therapy. The stability to trypsin and proteinase K degradation depends on the location of the exposed KL pair of L-amino acids. Indeed, only peptides that have a triplet of the L-amino acids *X*KL (where *X* denotes Leu or Lys) were fully degraded by the enzyme (Table I) (2). The amino acid sequence was scrambled, and the hydrophobic and hydrophilic amino acids were dispersed along the peptide chain. Interestingly, even such a major alteration did not significantly affect the potency and the spectrum of activity of the resulting Scrambled-4L and Scrambled-4D peptides but made the diastereomer less susceptible to enzymatic degradation. The ATR-FTIR studies revealed that their structure in the membrane has significant similarity to that of Amphipathic-2D and -3D despite the major difference in their sequences. This might partly explain why they all have similar activity. As stated before, because of the different distribution of the amino acids in this peptide compared with the amphipathic peptides, its antigenicity should also be different (3). The hydrophobic and positively charged amino acids were grouped. Unexpectedly, the resulting diastereomers maintained potent antimicrobial activity, although to a narrower spectrum of bacteria. Furthermore, Segregated-5D became inert to enzymatic degradation (Table I).

To determine whether the bacterial membrane is the target

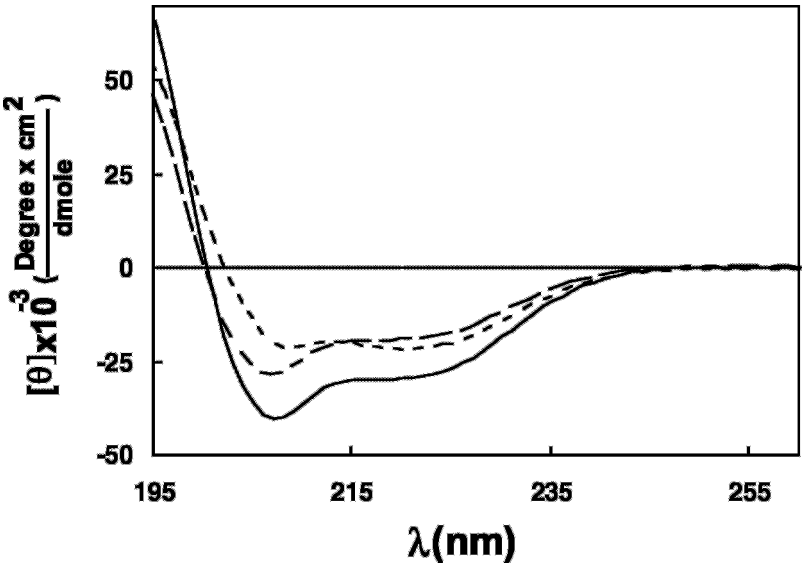

FIG. 6. **CD spectra of the all L-amino acid peptides.** The spectra were taken at 50 μM peptide dissolved in 1% SDS. *Solid line*, Amphipathic-1L; *dotted line*, Scrambled-4L; *dashed line*, segregated-5L.

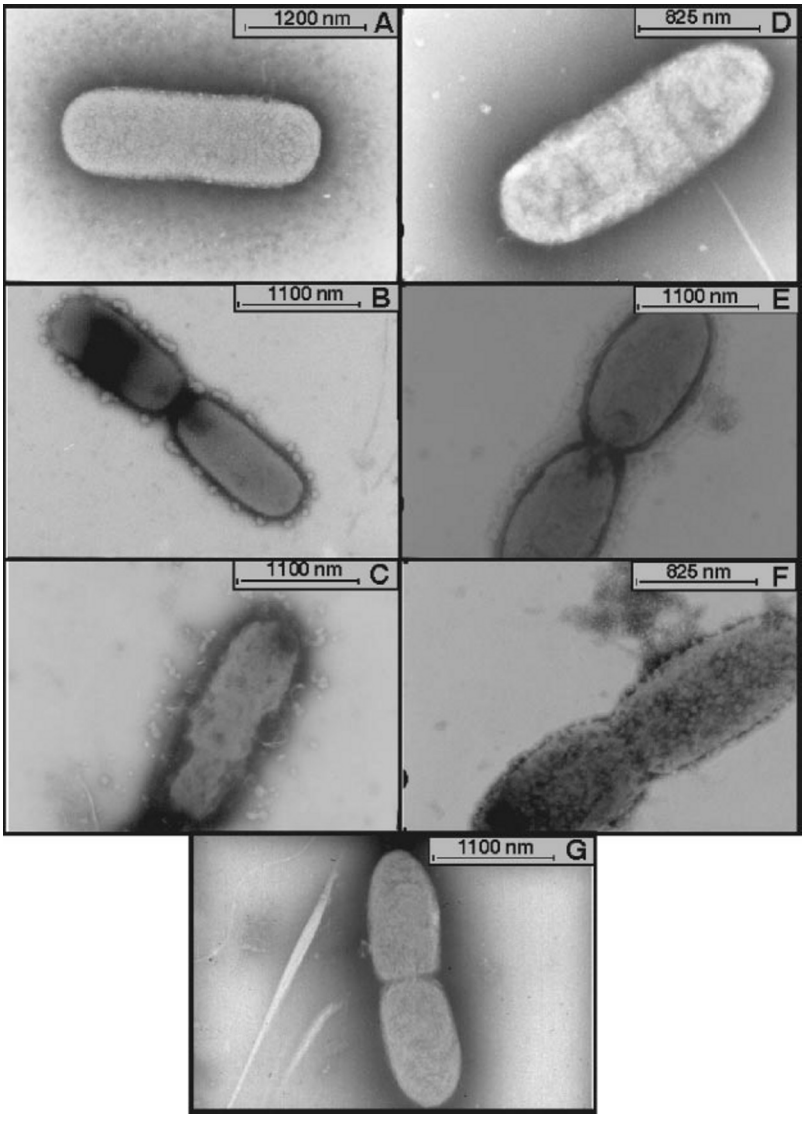

FIG. 7. **Electron micrographs of negatively stained *E. coli* D21 and *P. aeruginosa* left untreated and treated with the diastereomers at 60% MIC and at their MIC.** *A*, untreated *E. coli*. *B*, *E. coli* after treatment with Amphipathic-1D (60% of MIC). *C*, *E. coli* after treatment with Amphipathic-1D (at MIC). *D*, untreated *P. aeruginosa*. *E*, *P. aeruginosa* after treatment with Amphipathic-1D (60% of MIC). *F*, *P. aeruginosa* treated with Amphipathic-1D (at MIC). *G*, *P. aeruginosa* treated with Segregated-5D at the same concentration as indicated in *E*.

of all of the diastereomers studied here, we tested their ability to increase the permeability of model membranes mimicking the composition of the bacterial membrane and the outer leaflet of hRBC membranes. We found that all of the diastereomeric peptides have similar potencies in increasing the permeability of negatively charged vesicles (Fig. 2*A*). This result was not expected considering the major alteration of the distribution of the amino acids and the structure of the diastereomeric pep-

tides. One possible explanation is that grouping of the hydrophobic amino acids renders the peptide more hydrophobic. This is evident by the increasing retention time of the two segregated diastereomeric peptides compared with the others as seen by using RP-HPLC (Table I). This increase in hydrophobicity might compensate for the lack of amphipathic structure.

In contrast to the similar potencies of the diastereomers in increasing the permeability of PE/PG membranes, their spectrum of antimicrobial activity is different. To find a possible explanation for these differences, the diastereomers were also tested for their ability to dissipate the transmembrane potential of intact *S. aureus* and the spheroplasts of two *E. coli* strains that have different susceptibilities to the diastereomeric peptides (Table II). Importantly, we found a direct correlation between the MICs of the diastereomers toward *S. aureus* and their dose-dependent activity in dissipating the transmembrane potential of this bacterium (Fig. 3). However, we could not perform similar experiments with intact *E. coli*, because of difficulties in bringing the fluorescent dye into the inner membrane, and therefore we used spheroplasts of *E. coli*. We found that all of the diastereomers have similar activities toward the spheroplasts of the two species of *E. coli* (Fig. 4). This suggests that the differences in their activities result from their different abilities to diffuse through the outer membrane of Gram-negative bacteria, which depends on their structure. However, once the peptides cross the outside membrane, they have similar activities in the permeation of the cytoplasmic membrane.

Similar to many native antimicrobial peptides, the diastereomers were not hemolytic up to the maximal concentration tested (100 μM) (Table II), despite the fact that all of them (besides Segregated-6D) also permeate zwitterionic membranes, although about 10-fold less efficient than negatively charged membranes (Fig. 2*B*). Human erythrocytes are rich with negatively charged sialic acid-containing carbohydrate moieties in the form of glycoproteins and glycosphingolipids, which form the glycocalix layer. It is possible that the peptides stick to the negatively charged glycocalix layer, and because of their low partitioning capacity with the zwitterionic membranes, they cannot diffuse into the membrane.

In summary, the experiments presented here demonstrated that sequence alteration of lysine- and leucine-containing peptides maintains full or partial antimicrobial activity in both the all L-amino acid or the diastereomeric forms, however, with greater advantages for the diastereomers. Furthermore, once an active diastereomeric peptide was developed, the distribution of its amino acids could be tolerated to create a larger repertoire of diastereomeric peptides with improved properties that make them potential candidates for systemic drug use. In support of this we found in a preliminary study[2] that mice infected intravenously with *P. aeruginosa* and then treated intravenously for a few days with Amphipathic-1D were fully recovered (5 of 7), similarly to those treated with gentamicin (6 of 7). In contrast, all untreated mice or those treated with Amphipathic-1L died after 2 days. With regard to their mode of action, the data suggest that they act directly on the bacterial membrane, although additional targets are possible, as suggested for some native antimicrobial peptides (55). Their selectivity toward different species of bacteria is probably due to difficulties in diffusing through the outer layer into the inner bacterial membrane.

[2] N. Papo, Z. Oren, U. Pag, H.-G. Sahl, and Y. Shai, unpublished results.

REFERENCES

1. Boman, H. G. (1995) *Annu. Rev. Immunol.* **13,** 61–92
2. Russell, P. E., Milling, R. J., and Wright, K. (1995) in *Fifty Years of Antimicrobials: Past Perspectives and Future Trends* (Hunter, P. A., Darby, G. K., and Russell, N. J., eds) pp. 67–85, Cambridge University Press, Cambridge, UK
3. Lehrer, R. I., and Ganz, T. (1999) *Curr. Opin. Immunol.* **11,** 23–27
4. Hancock, R. E., and Diamond, G. (2000) *Trends Microbiol.* **8,** 402–410
5. Steiner, H., Hultmark, D., Engstrom, A., Bennich, H., and Boman, H. G. (1981) *Nature* **292,** 246–248
6. Zasloff, M. (1987) *Proc. Natl. Acad. Sci. U. S. A.* **84,** 5449–5453
7. Mor, A., Nguyen, V. H., Delfour, A., Migliore, S. D., and Nicolas, P. (1991) *Biochemistry* **30,** 8824–8830
8. Falla, T. J., Karunaratne, D. N., and Hancock, R. E. W. (1996) *J. Biol. Chem.* **271,** 19298–19303
9. Shai, Y. (1999) *Biochim. Biophys. Acta* **1462,** 55–70
10. Segrest, J. P., De, L. H., Dohlman, J. G., Brouillette, C. G., and Anantharamaiah, G. M. (1990) *Proteins* **8,** 103–117
11. Oren, Z., and Shai, Y. (1998) *Biopolymers* **47,** 451–463
12. Tossi, A., Sandri, L., and Giangaspero, A. (2000) *Biopolymers* **55,** 4–30
13. Blondelle, S. E., and Houghten, R. A. (1992) *Biochemistry* **31,** 12688–12694
14. Bessalle, R., Haas, H., Goria, A., Shalit, I., and Fridkin, M. (1992) *Antimicrob. Agents Chemother.* **36,** 313–317
15. Lee, S., Mihara, H., Aoyagi, H., Kato, T., Izumiya, N., and Yamasaki, N. (1986) *Biochim. Biophys. Acta* **862,** 211–219
16. Chen, H. C., Brown, J. H., Morell, J. L., and Huang, C. M. (1988) *FEBS Lett.* **236,** 462–466
17. Gazit, E., Lee, W. J., Brey, P. T., and Shai, Y. (1994) *Biochemistry* **33,** 10681–10692
18. Pouny, Y., and Shai, Y. (1992) *Biochemistry* **31,** 9482–9490
19. Strahilevitz, J., Mor, A., Nicolas, P., and Shai, Y. (1994) *Biochemistry* **33,** 10951–10960
20. Andreu, D., Merrifield, R. B., Steiner, H., and Boman, H. G. (1985) *Biochemistry* **24,** 1683–1688
21. Mignogna, G., Simmaco, M., Kreil, G., and Barra, D. (1993) *EMBO J.* **12,** 4829–4832
22. Barra, D., and Simmaco, M. (1995) *Trends Biotechnol.* **13,** 205–209
23. Kreil, G. (1997) *Annu. Rev. Biochem.* **66,** 337–345
24. Prenner, E. J., Lewis, R. N., Neuman, K. C., Gruner, S. M., Kondejewski, L. H., Hodges, R. S., and McElhaney, R. N. (1997) *Biochemistry* **36,** 7906–7916
25. Shai, Y., and Oren, Z. (1996) *J. Biol. Chem.* **271,** 7305–7308
26. Avrahami, D., Oren, Z., and Shai, Y. (2001) *Biochemistry* **40,** 12591–12603
27. Merrifield, R. B., Vizioli, L. D., and Boman, H. G. (1982) *Biochemistry* **21,** 5020–5031
28. Kliger, Y., Aharoni, A., Rapaport, D., Jones, P., Blumenthal, R., and Shai, Y. (1997) *J. Biol. Chem.* **272,** 13496–13505
29. Sims, P. J., Waggoner, A. S., Wang, C. H., and Hoffmann, J. R. (1974) *Biochemistry* **13,** 3315–3330
30. Loew, L. M., Rosenberg, I., Bridge, M., and Gitler, C. (1983) *Biochemistry* **22,** 837–844
31. Shai, Y., Bach, D., and Yanovsky, A. (1990) *J. Biol. Chem.* **265,** 20202–20209
32. Wu, M., Maier, E., Benz, R., and Hancock, R. E. (1999) *Biochemistry* **38,** 7235–7242
33. Yanagida, N., Uozumi, T., and Beppu, T. (1986) *J. Bacteriol.* **166,** 937–944
34. Oren, Z., and Shai, Y. (2000) *Biochemistry* **39,** 6103–6114
35. Surewicz, W. K., Mantsch, H. H., and Chapman, D. (1993) *Biochemistry* **32,** 389–394
36. Greenfield, N., and Fasman, G. D. (1969) *Biochemistry* **8,** 4108–4116
37. Wu, C. S., Ikeda, K., and Yang, J. T. (1981) *Biochemistry* **20,** 566–570
38. Schiffer, M., and Edmundson, A. B. (1967) *Biophys. J.* **7,** 121–135
39. Verkleij, A. J., Zwaal, R. F., Roelofsen, B., Comfurius, P., Kastelijn, D., and Deenen, L. V. (1973) *Biochim. Biophys. Acta* **323,** 178–193
40. Sawyer, J. G., Martin, N. L., and Hancock, R. E. (1988) *Infect. Immun.* **56,** 693–698
41. Ghosh, J. K., Shaool, D., Guillaud, P., Ciceron, L., Mazier, D., Kustanovich, I., Shai, Y., and Mor, A. (1997) *J. Biol. Chem.* **272,** 31609–31616
42. Feder, R., Dagan, A., and Mor, A. (2000) *J. Biol. Chem.* **275,** 4230–4238
43. Jackson, M., and Mantsch, H. H. (1995) *Crit. Rev. Biochem. Mol. Biol.* **30,** 95–120
44. Frey, S., and Tamm, L. K. (1991) *Biophys. J.* **60,** 922–930
45. Oren, Z., Hong, J., and Shai, Y. (1999) *Eur. J. Biochem.* **259,** 360–369
46. Hong, J., Oren, Z., and Shai, Y. (1999) *Biochemistry* **38,** 16963–16973
47. Sharon, M., Oren, Z., Shai, Y., and Anglister, J. (1999) *Biochemistry* **38,** 15305–15316
48. Tatulian, S. A., Biltonen, R. L., and Tamm, L. K. (1997) *J. Mol. Biol.* **268,** 809–815
49. Rothschild, K. J., and Clark, N. A. (1979) *Science* **204,** 311–312
50. Dwivedi, A. M., and Krimm, S. (1984) *Biopolymers* **23,** 923–943
51. Pezolet, M., Bonenfant, S., Dousscau, F., and Papineau, Y. (1992) *FEBS Lett.* **299,** 247–250
52. Mantsch, H. H., Perczel, A., Hollosi, M., and Fasman, G. D. (1993) *Biopolymers* **33,** 201–207
53. Byler, D. M., and Susi, H. (1986) *Biopolymers* **25,** 469–487
54. Miyazawa, T. (1960) *J. Mol. Spectrosc.* **4,** 168–172
55. Zhang, L., Scott, M. G., Yan, H., Mayer, L. D., and Hancock, R. E. (2000) *Biochemistry* **39,** 14504–14514